14,15

Formation of kink pairs in the generalized Hirth–Lothe model

© B.V. Petukhov

Shubnikov Institute of Crystallography of Federal Scientific Research Centre „Crystallography and Photonics“ of Russian Academy of Sciences,
Moscow, Russia

E-mail: petukhov@crys.ras.ru

Received October 13, 2024
Revised February 1, 2025
Accepted February 2, 2025

The kinetics of kink pair formation on dislocations is described within the framework of a model intermediate between the sharp kink model and the continuum elastic string model. The effects resulting from the discrete structure of crystalline materials are considered. The theory is based on the universal Frenkel–Kontorova model and can be applied to extended systems of various natures.

Keywords: dislocation kinks, Peierls barriers, Frenkel–Kontorova model, energy landscape.

DOI: 10.61011/PSS.2025.02.60691.261

1. Introduction

Kinetics of transitions of many extended linear systems between degenerate multistable states in potential profiles plays an important role in numerous problems in physics, chemistry, biology, etc.: in step motion on growing crystal surface, in biological macromolecules, nanowires, magnetization switching in spin chains and molecular chain-structure magnetic materials and many other one–dimensional and quasi-one-dimensional structures [1–3]. In particular, the study of dislocation glide in a periodic potential profile of lattices known as the Peierls barriers has a long history [4–6]. Due to the extension of the range of promising materials, having high crystal profile, for high temperature and microelectronic applications, investigation of dislocation kinetics in the Peierls barriers has been increasingly important and the number of corresponding studies is quickly growing. Here are just a few reviews as an example [7–15].

Decay of metastable states of extended systems, dislocation is chosen as a prototype in this work for clarity, occurs through the fluctuation formation of energetically preferable state nuclei that are transformed into kink pairs at later stages. Kinks are boundaries between various states, or domains. Many studies use various approaches to calculate the kink pair formation kinetics; due to countless number of such studies, only references to monographs and reviews will be given. A continual approach, that describes kinks as topological solitons, is popular [16–20]. Capability of obtaining precise analytical descriptions of kink properties in some cases serves as an incentive [21,22]. At the same time, continual approaches with regard to solid bodies are approximate due to lattice discreteness and need a special justification. This often reduces to the selection of a special parameter range. Extension of the parameter range is achieved by considering the discreteness effect according to the perturbation theory at the limit where its effect is low [23,24].

However, there are situations where discreteness has a significant effect on the kink properties [25,26]. For example, kinks on dislocations in silicon or germanium type semiconductors, that have been a subject of experimental and theoretical investigations for many years [27–31], have a short length in the order of a lattice period and perceive the lattice discreteness to a full extent. Translation invariance discontinuity is an evident medium discreteness effect. Kink energy varies on a periodic basis as the kink moves along a system with a lattice constant. Energy difference between potential maxima $E_{\max}$ and minima $E_{\min}$ for kinks $\Delta E_{P2} = E_{\max} - E_{\min}$ is called the Peierls barriers of the second kind, as opposed to the Peierls barriers of the first kind for a dislocation as a whole. Periodic energy potential profile of the first kind is often described as will be used below by the harmonic law $E_P(y) = E_0 \cos(2\pi y/h)$, where $E_0 = \sigma_P bh/2\pi$ is the typical energy per dislocation length unit; σ_P is the Peierls stress, which, when exceeded, leads to removal of the barriers against the dislocation motion; b is the Burgers vector value; h is the kink height equal to a distance between the potential minima; y is the coordinate in the dislocation motion direction. When an external driving force does not exist or is relatively low, kinks get a static configuration corresponding to the energy minimum. Kink may move only when the activation barriers are overcome using thermal and quantum fluctuations.

There is a theory of thermally activated dislocation motion according to the Lothe and Hirth mechanism. This theory is opposed to continual models [32]. This theory treats kinks as a structureless sharp boundaries of system domains being in various states, in particular, in various crystal valleys. The Lothe-Hirth model was successfully used to describe the dislocation dynamics in silicon or germanium type semiconductors [33]. This theory neglects the modification of kink and barrier configurations at kink migration under the driving force. Due to its simplicity, this theory served as a convenient reference point for describing additional effects, for example, those related to quantum tunneling [34] and point defect effect [35–38]. However, non-consideration of the external load effect on

kink parameters limits the applicability of this ultradiscrete approach by a low driving force region where the energy difference between various degenerate states is low. In a more general case, it should be considered that, when an external driving force is applied, degeneracy of states is removed and the potential profile takes a form of an inclined „washboard", as it is often called for clarity.

In continuous medium, any external force is sufficient to set the kink in motion, but in the discrete case this is not true. When the external force is relatively low, a kink changes its configuration a little, but is still static at minimum of the potential. However, the potential maximum and minimum energies vary, the distance between them decreases with decreasing driving force and vanishes at some critical value. With a high driving force, there are no static kink confgurations, and dynamic mode is implemented. Thus, the Lothe–Hirth theory requires generalization both to consider the dependence of activation parameters on the driving force and to describe the transition between the static and dynamic kink behavior. This work develops a more general theory that offers a more in-depth study of kink energy at various kink formation process stages.

2. Kink generation

The Lothe-Hirth model defines the kink pair nucleus as a dislocation segment that has moved from the initial potential minimum extended along a crystallographic direction to a neighboring minimum limited by sharp inflections (the kink and its twin antikink). The force $F = \sigma b$ acts per unit dislocation length in a uniform stress field σ. Kink pair energy is written as $E_{\mathrm{kpHL}} = 2E_{\mathrm{k}} - Fhx$, where E_{k} is the single kink or antikink energy in the absence of a driving force, x is the size of the transferred segment. With a low driving force, the size of nuclei, that are substantial for thermally activated transitions, is large and the interaction between the limiting them kink and antikink is neglected. The kink pair is considered as a stable formation, if the energy reduction on the pair size exceeds the thermal energy $k_{\mathrm{B}}T$, which takes place at $x > k_{\mathrm{B}}T/Fh$, and a sufficient barrier is opposed to thermal fluctuations that can collapse the pair, i. e. lead to twin kinks annihilation. The Lothe-Hirth theory is, in fact, one-dimensional and considers only one degree of freedom — coordinate of an invariant-shape kink along the dislocation line. This is not sufficient to fully describe the dependence of activation parameters on the driving force.

Let's describe kink formation in the improved model compared with the model used in the Lothe–Hirth theory. The classical Frenkel–Kontorova model serves as a suitable tool to describe the discrete kink energy [39]. This model addresses a chain of particles or links that is periodic along one direction, e. g. x. These particles or links are hereinafter also referred to as „atoms" for brevity. The period is denoted as a. Atoms are interconnected by elastic forces and are in the orthogonal direction y in a potential profile hereinafter referred to as the substrate potential. For illustrative calculations, a harmonic profile deformed by a uniform stress field will be taken as the substrate potential in this study. Various chain configurations are given by a set of atomic displacements along the y — $\{y_n\}$ axis counted from the ground state in the substrate potential minimum.

Chain energy at any atom configuration using dimensionless parameters is written as

$$E_{\mathrm{FK}} = \sum_n \left[\frac{\beta}{2} (u_{n+1} - u_n)^2 + 1 - \cos(u_n) - E u_n - E_{\mathrm{m}} \right], \tag{1}$$

where n is the sequence number of atoms along the chain, β sets the scale of elastic interaction between atoms, $u_n = 2\pi y_n/h$, y_n is the displacement of the n-th atom from the ground state of the chain at $u_{\mathrm{m}} = \arcsin(E)$ (here, m defines a minimum, not to be confused with a sequence number), $1 - \cos(u_{\mathrm{n}}) - E_{u_n}$ is the substrate potential normalized (as E_{FK}) to the typical energy $E_0 = \sigma_{\mathrm{P}} abh/2\pi$, $E = \sigma/\sigma_{\mathrm{P}}$ characterizes the driving force, $E_{\mathrm{m}} = 1 - \cos(u_{\mathrm{m}})$ — $E u_{\mathrm{m}}$ is the ground state energy falling on one period and also normalized to E_0.

Expression (1) sets the energy landscape in the configuration space, whose dimension is equal to an unlimitedly large number of atoms in the chain. With $E < 1$, there are minima and minima in this landscape; chain positions along the maxima are metastable states at $1 > E > 0$. Energetically favorable chain configurations defined by extremum conditions are of principal interest

$$dE_{\mathrm{FK}}/du_n = -\beta(u_{n+1} + u_{n-1} - 2u_n) + \sin(u_n) - E = 0. \tag{2}$$

At high $\beta > 1$, i. e. at high bond rigidity, relative displacements of neighboring atoms are small, and system of equations (2) changes to its continual equivalent describing an elastic string:

$$\beta a^2 \cdot \frac{d^2 y}{dx^2} - \sin(u) + E = 0. \tag{3}$$

β is related to the linear string tension coefficient κ by $\beta = \kappa h/2\pi\sigma_{\mathrm{P}} b a^2$. In the absence of the driving force $E = 0$, equation (3) is a well known static sine-Gordon equation [40] whose exact solution is a kink soliton with $E_{\mathrm{k}} = 8\beta^{1/2}$. Equation (3) is also easily solved when there is a driving force, thus, allowing the calculation of, in particular, saddle-point configurations at the barrier top for system transition between the potential valleys [41]. Energy of such configuration is the kink pair activation energy equal to

$$E_{\mathrm{kp}} = 2 \int_{u_{\mathrm{m}}}^{u_{\mathrm{Max}}} \sqrt{2\beta[\cos(u_{\mathrm{m}}) - \cos(u) + E(u_{\mathrm{m}} - u)]}\, du, \tag{4}$$

where u_{Max} is the maximum displacement in the saddle-point configuration that corresponds to the integrand positivity boundary in (4) and is defined by condition $\cos(u_{\mathrm{m}}) - \cos(u_{\mathrm{Max}}) + E(u_{\mathrm{m}} - u_{\mathrm{Max}}) = 0$. Equation (4) may be approximated by a simple equation

$E_{kp} \approx 2E_k(1-E)^{1.3}$. Analytical study of the asymptotic dependence of activation energy (4) at high driving forces was carried out in [42].

There are numerous studies that approximately describe discrete kinks as perturbed kink solitons of the sine-Gordon equation [23,24]. Perturbation may be considered as low, when a kink length is long compared with the chain period. When the kink size is comparable with the period, discreteness is perceived to a full extent and cannot be considered as low perturbation. In this case, another approach shall be used to solve system of equations (2) and describe kink configurations. Such effective and extremely vivid approach, which is more flexible than the Lothe–Hirth theory, was proposed in [43–46] and used primarily to study the properties and dynamics of individual kinks. This work will use the same approach to describe the kink pair formation kinetics. In the framework of this approach, some idea about the energy landscape arrangement may be get by examining landscape projections with arbitrarily given displacements of some atoms, and considering the displacements of the rest atoms as adapting to them with fulfillment of relations (2). Thus, the configuration space dimension may be reduced effectively by considering partly equilibrium chain states. At low values of β, elastic atom bonds are easily extendable and relative atomic displacements may be quite large. As a result, a kink between neighboring crystal profile valleys will strain bonds only between few atoms. As it will be confirmed by further calculation, only one or two boundary atoms may be prone to considerable displacement, and other atoms may be displaced from the ground state u_m or $u_m + 2\pi$ not too much and their equilibrium positions can be easily calculated according to the perturbation theory. Considerably displaced atoms will be referred to as active centers. Consideration of their displacements, that vary with the driving force variation, provides the model with a degree of structure, which is absent in the Lothe–Hirth theory and makes it possible to go beyond this theory and address additional effects.

At high energy of elastic interaction between atoms in the kink compared with the thermal energy k_BT, low-energy states of the chain contain straight-line portions that are extended with respect to the period and are located in the substrate potential minima. The study will focus on fluctuationally formed chain configurations that have such straight-line portion as an initial state. Atoms that are slightly displaced from the equilibrium positions u_m or $u_m + 2\pi$ are in the neighborhood where the substrate potential is close to the quadratic potential. Thus, system of equations (2) may be linearized with respect to the displacements $\delta u_n = u_n - \arcsin(E)$: $-\beta(\delta u_{n+1} + \delta u_{n-1} - \delta u_n) + (1-E)^{1/2}\delta u_n = 0$. We find solution in the form of $\delta u_n \propto B\lambda^n$; its substitution into the linearized equations taking into account the finiteness at $n \to \infty$ gives

$$\lambda = 1/\Big\{1 + (1-E^2)^{1/2}2\beta + \left[(1-E^2)/4\beta^2 + (1-E^2)^{1/2}/\beta\right]^{1/2}\Big\}. \quad (5)$$

Kinks are formed by pairs when passing through symmetric saddle-point configurations, where only atomic displacements at nucleus boundaries will be considered as significantly displaced from equilibrium positions. Due to the symmetry, the kink pair energy may be written as a doubled sum over positive atom numbers:

$$E_{kp} = 2\sum_{n=0}^{N}\left[\frac{\beta}{2}(\delta u_{n+1} - \delta u_n)^2 + (1-E^2)^{1/2} - \cos(u_n) - E\delta u_n\right]. \quad (6)$$

In the simplest case, only the first atom with number 0 is considered as active and will be exactly addressed, the rest atoms are considered to be in a quadratic neighborhood of the potential profile and optimally adapted to δu_0. By substituting their equilibrium displacements $\delta u_n = \delta u_0 \lambda^n$ in (6), we obtain approximately

$$E_{kp} \approx \delta u_0^2\Big\{\beta(1-\lambda)^2 + (1-E^2)^{1/2}\lambda^2/(1-\lambda^2)\Big\} + 2(1-E^2)^{1/2}\left[1-\cos(\delta u_0)\right] - 2E\sin(\delta u_0) - 2E\delta u_0. \quad (7)$$

Expression (7) gives an approximate one-dimensional representation of the energy profile, in which the kink pair nucleus evolves at the initial formation stage. Different behavior of the initial stage and the barriers to be overcome depending on the magnitude of the driving force are illustrated in Figure 1. It shows the kink pair energy variation along the adiabatic path, on which displacements of all other chain atoms were adapted to the active atom position, for various values of E. Rigidity parameter of elastic atomic bonds is $\beta = 0.05$. Energy of a chain with a kink pair in the first minimum is higher than the ground state energy when $E < E_{cr} = 0.1428\ldots$ and lower when $E > E_{cr}$. In the latter case, the barrier height for inclusion into the first minimum is the kink pair activation energy because return to the initial state, i.e. annihilation, or kink collapse, is unlikely. In the former case, the state in this minimum is only intermediate and the next barriers shall be overcome for irreversible formation of a kink pair before the falling in a negative-energy minimum.

Calculation result of E_{cr} for any values of β may be approximated by means of fitting by $E_{cr} \approx 2.2637\beta^{0.9}/(1+1.6\beta)$, as it is demonstrated in Figure 2.

After overcoming the first barrier and falling in the nearest minimum, a fork with various evolution options is possible. To get a fuller picture, it is useful to generalize the calculation a little and consider two atoms as active ones by including also atom 1 in them. Atoms with large numbers $n > 1$ are considered to be adapted to the displacement of atom 1 — δu_1 as $\delta u_n = \delta u_1 \lambda^{n-1}$. In this case, infinite-dimensional energy landscape (1) or (6) reduces to a vivid two-dimensional one, being a function of two variables δu_0 and δu_1.

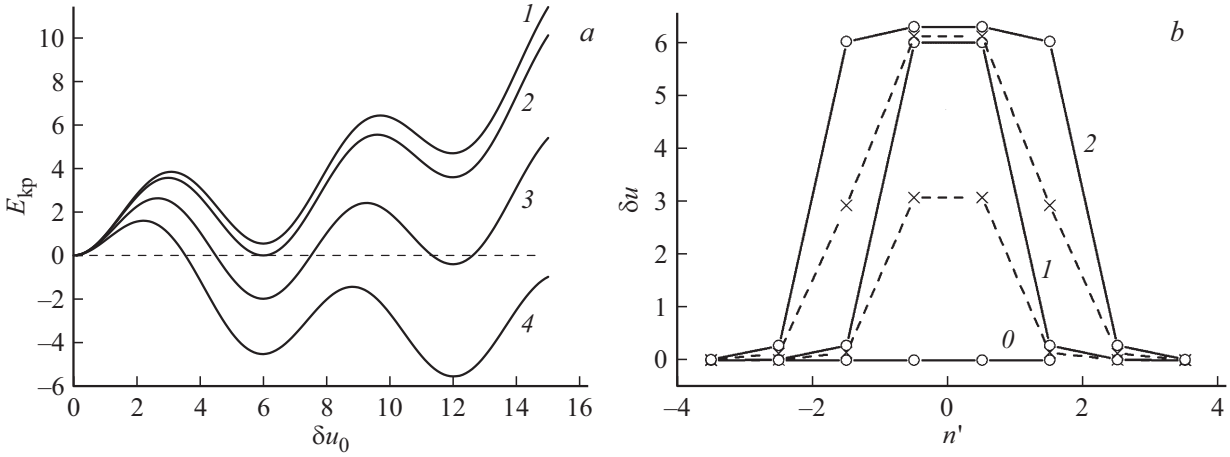

Figure 1. *a*) Dependence of the kink pair energy on the active atom position at various driving forces. Curve *1* corresponds to $E = 0.1$, *2* — $E = E_{cr} = 0.1428\ldots$, *3* — $E = 0.3$, *4* — $E = 0.5$. $\beta = 0.05$. *b*) Chain configurations in extreme points of the energy landscape. Circles show atomic displacements in minima, crosses show atomic displacements in saddle points.

Without giving explicitly an analytical expression derived apparently from (1), the situation will be illustrated by a vivid picture. Such landscape with parameters $\beta = 0.05$ and $E = 0.1$ is illustrated in Figure 3 using energy level lines. Energies, to which the shown level lines are related, are defined primarily by the heights of saddle points through which they pass. Dashed lines show the adiabatic curves corresponding, with the set value of δu_0, to the energy minimum over the displacements of all other atoms, including atom 1, and described by foregoing expression (7). Descriptive-geometrical view of such line is represented by the bottom of a valley going through a saddle point from one profile minimum to another. Minima correspond to stables or metastable chain states, and the energy difference in a saddle point and minimum gives the barrier height for transition from one state to another.

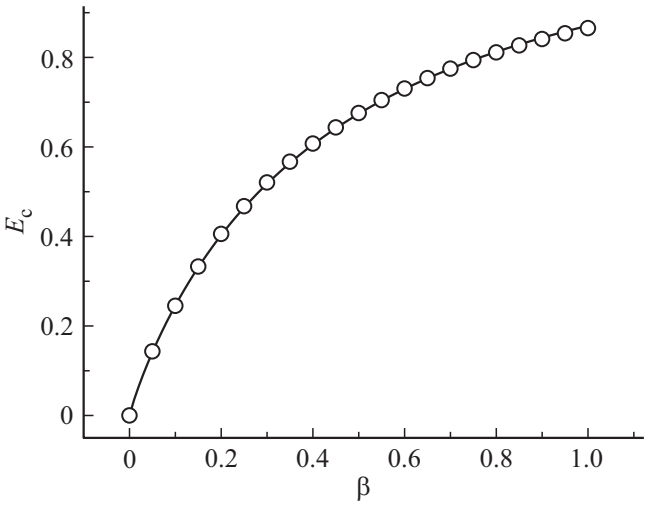

Figure 2. Dependence of a boundary driving force, that corresponds to the occurrence of a chain state with a lower energy than the initial state, on the rigidity parameter of elastic bonds β (circles). Solid line shows the result of fitting by the analytical expression $E_{cr} \approx 2.2637\beta^{0.9}/(1 + 1.6\beta)$.

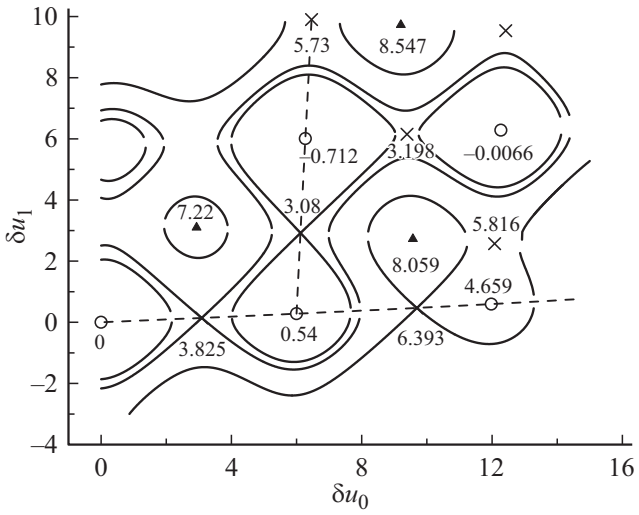

Figure 3. Two-dimensional energy landscape in the displacement space of the first atoms δu_0 and δu_1 with $\beta = 0.05$ and $E = 0.1$ shown by the constant energy level lines. Circles show the minima, triangles show the maxima, crosses show the saddle points. Dashed lines show the valleys going between minima through saddle points.

3. Initial propagation stage of kinks composing in a pair

When the external driving force is present, all chains are metastable, and thermal fluctuations give rise to chain evolution in a direction determined by the driving force to lower energy states. Basically, such evolution may occur in various ways through different consecutive energy minima. However, due to the abrupt Arrhenius dependence

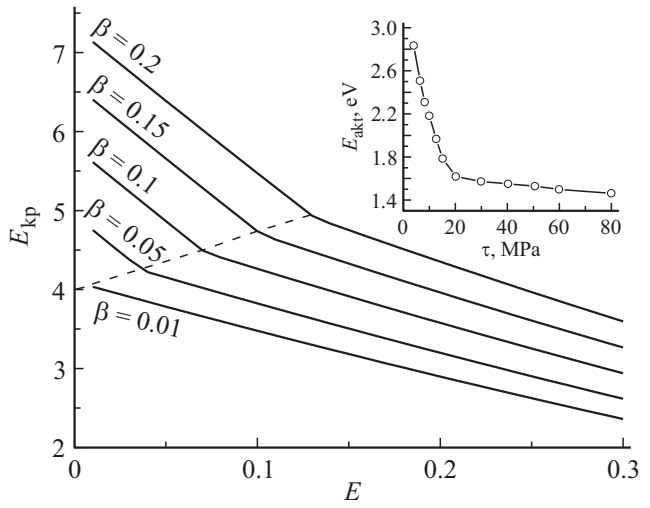

Figure 4. Dependence of the kink pair activation energy on the driving force at different values of β marked by numbers at the curves. The activation energy at higher driving forces is defined by a barrier for transition from the ground state to the first potential minimum, and at lower driving forces — by a barrier for transition from the first minimum to the second one. For comparison, the inset shows the dependence of dislocation motion activation energy on stress in Ge [31].

of transition rates on barrier heights, a transition will most probably take place through the lowest saddle point on the profile. Thus, in the case illustrated in Figure 3, after the initial transition to the minimum with the energy of 0.54, predominant transitions to a minimum with the energy of 0.712 through a saddle point with the height of 3.08, rather than to a minimum with the energy of 4.659 through a saddle point with the height of 6.393, may be expected.

Transition from the initial state marked with 0 to the nearest energy minimum 0.54 with configuration marked with 1 may be considered as a metastable kink pair initiation stage. Transition from this state to the minimum -0.712 through a saddle point with the height of 3.08 is the start of expansion of the kink pair nucleus, which will be discussed below.

Figure 4 shows the dependence of the kink pair activation energy on the driving force at different values of β. This dependence in different driving force regions (on different sides of the dashed line in the figure) along the adiabatic lines is defined by various transitions, due to which it is represented by curves with kinks. The activation energy at higher driving forces is defined by a barrier for transition from the ground state to the first potential minimum; the activation energy at lower driving forces is defined by a barrier for transition from the first minimum to the second one. As shown in Figure 4, the barrier for kink pair formation in a wide region depends considerably from the driving force and decreases as the driving force increases. For qualitative comparison, the inset shows the dependence of the activation energy on the driving force found from the dislocation rate measurements in Ge [31].

4. Formation of kink pairs with various sizes

To describe the kink pair nucleation stages that follow the initiation stage, energies of wider nuclei, whose boundaries are extended farther from the central atom, will be studied. Transitions to them are energetically more favorable than further movement of the central atom because such movement is prevented by tension forces from two neighboring atoms. Displacement of the boundary is prevented by oppositely directed tension forces, that partially compensate each other, from neighbors. Thus,the „activity“ baton shall be passed to atoms adjacent to the central atom, and atom 0 falls into a quadratic neighborhood of the second substrate potential valley and the displacement of this atom adapted to the displacement of atom 1 can be easily found and excluded from the further calculation: $\delta u_0 = 2\pi - \lambda(2\pi - \delta u_1)$. We obtain an energy profile as illustrated in Figure 5, that depends now on δu_1 and δu_2 and shall be studied identically to the previous profiles as shown in Figure 3 on the basis of equation (7). The main change from (7) is given by the energy difference between the second and first substrate valleys $-4\pi E$ introduced by a chain-period displacement of the nucleus boundaries.

Repeated nuclei expansion steps lead to further energy reduction in the minima mainly due to the contributions of the growing number of central atoms. We consider the kink pair nuclei containing $2k_0$ of the central atoms that have moved to the second substrate potential valley neighborhood. Active atoms with numbers $k = \pm k_0$ at the nucleus boundaries are considered. Atoms within the boundaries are in the quadratic neighborhood of the upper substrate potential minimum and have displacements $\delta u_{k_0-1} = 2\pi - \lambda(2\pi - \delta u_{k_0})$, $\delta u_k = 2\pi - \lambda^{k_0-k}(2\pi - \delta u_{k_0})$, $\delta u_{k'} = \delta u'_{k_0} \cdot \lambda^{k_0-k}$. Groove implies counting from the bottom of the upper substrate potential valley. Atoms with numbers from $k_0 + 1$ to ∞ are in

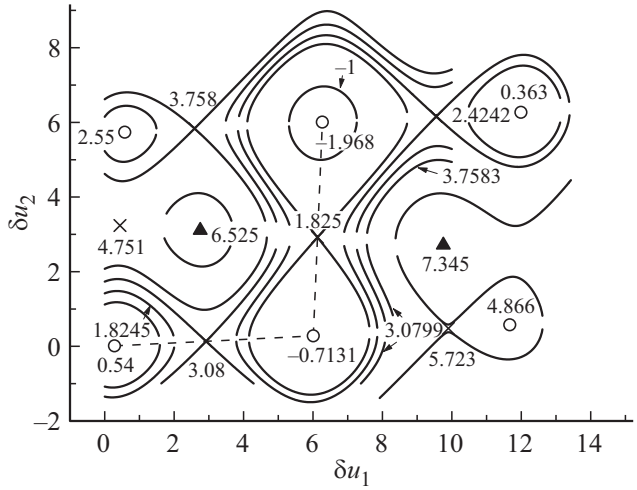

Figure 5. Energy profile for the kink pair nucleus evolution stage that follows the initiation stage with active atoms 1 and 2. Parameters are the same as in Figure 3: $\beta = 0.05$ and $E = 0.1$.

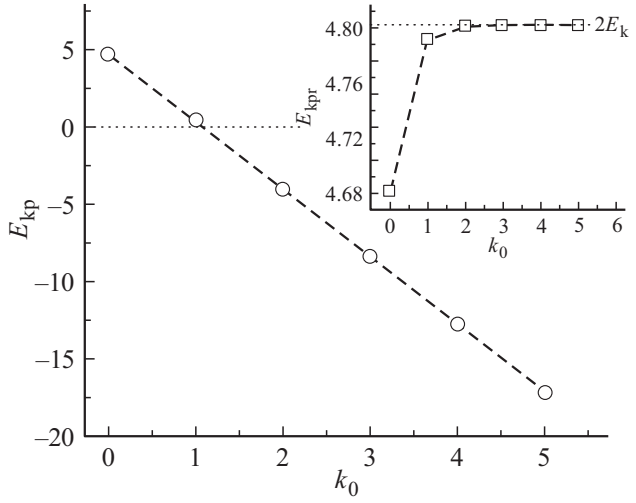

Figure 6. Minimum energies of kink pair nuclei with various sizes between the boundaries $-k_0$ and k_0. $\beta = 0.4$, $E = 0.35$. The inset shows the given values without considering the energy reduction in the second substrate potential valley.

the quadratic neighborhood of the lower substrate potential minimum and have displacements $\delta u_k = \delta u_{k_0}\lambda^{k-k_0}$.

Chain energy E_c is obtained by addition of the central atom energy to expression (7):

$$E_c = 2\sum_{n=0}^{k_0-1}\left[\frac{\beta}{2}(\delta u_{n+1} - \delta u_n)^2 + \cos(u_m) - \cos(u_n) - E\delta u_n\right]$$

$$= \beta u'^{\,2}_{k_0}\left[\beta(1-\lambda)^2 + (1-E^2)^{1/2}\lambda^2\right] \times \lambda^2(1-\lambda^{2k_0})/(1-\lambda^2) - 2\pi E k_0. \quad (9)$$

The obtained expression makes it possible to calculate the optimum energies of nuclei with various sizes on the energy profile that correspond to lower barriers for kink pair formation. Figure 6 illustrates the calculation data. For the chosen parameters, the nuclei energies with $k_0 = 0$ and 1 exceed the ground state energy and, therefore, are instable with respect to collapse. Nuclei with many central atoms $k_0 > 2$ have a lower energy than the ground state and tend to further expansion. A transition region around the boundary quickly achieves a standard shape and energy as the nucleus size increases, as demonstrated in the inset in Figure 6 that shows the minimum nucleus energy variation with the subtraction of the central part contribution $-4\pi k_0 E$. The rest portion of the nucleus energy being set may be assigned to two kinks, so the energy of a sufficiently wide nucleus is described by expression

$$E_{kp} = 2E_k - 2k_0\Delta E, \quad (10)$$

where $\Delta E = 2\pi E$ is the atom energy reduction in atom displacement between the substrate potential valleys. Equation (10) is identical to the corresponding expression in the Lothe–Hirth theory, but with the difference that the kink shape is not absolutely abrupt now because it is described by nonuniform displacements of the active and adjacent atoms that vary additionally with the varying driving force, on which the kink energy also depends.

5. Conclusion

The infinite-dimensional Frenkel–Kontorova model, that is quite complex for the quantitative analysis of the model behavior, is simplified drastically using two concepts. The first of them is the utilization of partly equilibrium system states where a small number of chain atoms occupy arbitrary positions in the potential profile, and the rest atoms are adiabatically adapted to them. As a result, the infinite-dimensional energy profile is reduced to any desired dimension. Approximation accuracy, that is generally justified at low rigidity of the elastic bonds between chain links, depends on the number of dimensions. The second concept implies that an optimum sequence of system transitions shall be chosen in the configuration space. Such choice among numerous fluctuationally available ways becomes almost unambiguous when the temperatures or, rather, thermal energies $k_B T$ are small compared with the typical barrier heights in the energy landscape. Though, generally speaking, in a relatively high driving force region, the probability of deviations from the main scenario with transitions only to the nearest substrate potential valley and of introduction of some fraction of more complex transitions cannot be completely excluded. For example, with formation of more energy-consuming „multilevel" kinks.

Utilization of these two concepts results in comparatively simple model described in [4,32] that makes it possible to expand the Lothe-Hirth theory and describe the kink pair formation kinetics in a much wider region of parameters where there is a considerable dependence of the activation energy on the driving force. Moreover, the model predicts the dependence behavior modification. According to the calculation as shown in Figure 3, the activation energy in a relatively high driving force region is defined by transitions from the system ground state to the nearest energy profile minimum. In a lower driving force region, the activation energy is defined by the initial expansion stage of a nucleus whose boundaries later take a typical shape of isolated kinks. As a result, large nuclei meet qualitatively the Lothe-Hirth theory, though in a modified and generalized form, because there is the dependence of the activation parameters on the driving force. As the rigidity of elastic bonds between the system links increases and more links are involved in the kink pair formation, this dependence gets smoothed and translates into continual limit (4). Thus, the proposed theory fills the gap in the knowledge about kink pair formation kinetics throwing a bridge between the Lothe-Hirth abrupt domain wall model and continual elastic string model.

Variation of the transition that controls the kink pair formation process in different ranges of values of the

driving force gives rise to a break in the dependence of the activation energy on the driving force as illustrated in Figure 4. A qualitatively similar break, which is reflected in the inset to Figure 3, was observed in experiments for dislocation motion rate measurement in Ge [31] and in other semiconductor materials [47–49].

Experimental data for direct dislocation rate measurements and activation parameters extracted from macroscopic mechanical tests of materials with kink plastic deformation mechanism demonstrates a wide variety. In metals with body-centered cubic lattice with a relatively low Peierls stress with respect to the shear modulus, there is a smooth dependence of the activation energy on load described by expression (4), though, often perturbed by the presence of other defects. In materials featuring high Peierls stresses, including semiconductors with covalent bonds between atoms, there is often no dependence of the activation energy on the external load in certain variation intervals in accordance with the Lothe-Hirth theory. However, in wider stress variation intervals, there are deviations from the theory predictions, for example, in Ge, InP and other semiconductors and materials with intermediate types of chemical atomic bonds [27–31,47–49]. Activation energies appear to be different in relatively higher and lower stress intervals, which is in qualitative agreement with the findings of this work.

Funding

This work was supported by the Ministry of Science and Higher Education within the State assignment FSRC „Crystallography and Photonics“ RAS.

Conflict of interest

The author declares no conflict of interest.

References

[1] One-Dimensional Nanostructures / Ed. Z.M. Wang. Springer, Science+Business Media, N.Y. (2008).
[2] A.S. Davydov. Soviet Physics Uspekhi. **25**, 898 (1982).
[3] M. Remoissenet. Waves Called Solitons: Concepts and Experiments. Springer, Berlin. (1994).
[4] J.P. Hirth, J. Lothe. Theory of Dislocations. McGraw-Hill (1967).
[5] U. Messerschmidt. Dislocation dynamics during plastic deformation / Ed. R. Hull. Berlin. Springer Science & Business Media, Heidelberg (2010).
[6] B.V. Petukhov. Dinamika dislokatsiy v kristallicheskom rel'efe. Dislokatsionnye kinki i plastichnost' kristallicheskikh materialov. Saarbrucken: Lambert Academic Publishing (2016). 385 s. (in Russian).
[7] C.R. Weinberger, G.J. Tucker, S.M. Foiles. Phys. Rev. B **87**, *5*, 054114 (2013).
[8] S.P. Fitzgerald. Sci. Rep. **6**, *1*, 39708 (2016). https://doi.org/10.1038/srep39708
[9] L. Dezerald, L. Proville, L. Ventelon, F. Willaime, D. Rodney. Phys. Rev. B **91**, *9*, 094105 (2015). https://doi.org/10.1103/PhysRevB.91.094105
[10] F. Maresca, W.A. Curtin. Acta Materialia **182**, 144 (2020). https://doi.org/10.1016/j.actamat.2019.10.007
[11] A. Ghafarollahi, W. Curtin. Acta Materialia **215**, 117078 (2021). https://doi.org/10.1016/j.actamat.2021.117078
[12] I.H. Kim, H.S. Oh, S.J. Kim, E.S. Park. J. Alloys. Compounds **886**, 161320 (2021). https://doi.org/10.1016/j.jallcom.2021.161320
[13] E.P. George, D. Raabe, R.O. Ritchie. Nature Rev. Mater. **4**, *8*, 515 (2019).
[14] Y. Tang, R. Wang, B. Xiao, Z. Zhang, S. Li, J. Qiao, S. Bai, Y. Zhang, P.K. Liaw. Progr. Mater. Sci. **135**, 101090 (2023). https://doi.org/10.1016/j.pmatsci.2023.101090
[15] I.J. Beyerlein, P. Cao, T.M. Pollock. Mater. Res. Soc. Bull. **48**, *7*, 746 (2023). https://doi.org/10.1557/s43577-023-00567-8
[16] R.K. Dodd, J.C. Eilbeck, J.D. Gibbon, H.C. Morris. Solitons and Nonlinear Wave Equations. Academic Press Inc. (1982).
[17] Y.S. Kivshar, B.A. Malomed. Rev. Mod. Phys. **61**, *4*, 763 (1989).
[18] A.R. Bishop, J.A. Krumhansl, S.E. Trullinger. Physica D **1**, *1*, 1 (1980).
[19] A. Scott. Nonlinear Science: Emergence and Dynamics of Coherent Structures. Oxford University Press, Oxford (2003).
[20] T. Vachaspati. Kinks and Domain Walls. An Introduction to Classical and Quantum Solitons. Cambridge University Press, Cambridge, N.Y., Melbourne, Madrid, Cape Town, Singapore, São Paulo (2006).
[21] The sine-Gordon Model and its Applications / Eds J. Cuevas-Maraver, P.G. Kevrekidis, F. Williams. Springer, Switzerland (2014).
[22] V.E. Zakharov, S.V. Manakov, S.P. Novikov, L.P. Pitaevski. Teoriya solitonov: Metod obratnoy zadachi. Nauka, M. (1980). 319 s. (in Russian).
[23] M.G. Clerc, R.G. Elías, R.G. Rojas. Philos. Trans. R. Soc. A **369**, *1935*, 412 (2011).
[24] M.J. Ablowitz, Z.H. Musslimani, G. Biondini. Phys. Rev. E **65**, *2*, 026602 (2002).
[25] D. Hennig, G.P. Tsironis. Phys. Rep. **307**, *5–6*, 333 (1999).
[26] M. Peyrard, M.D. Kruscal. Physica D **14**, *1*, 88 (1984).
[27] H. v. Schaumburg. Philos. Mag. **25**, *6*, 1429 (1972).
[28] V.I. Nikitenko, B.Ya. Farber, Yu.L. Iunin. JETP **66**, *4*, 738 (1987).
[29] Yu.L. Iunin, V.I. Nikitenko. Scripta Materialia **45**, *11*, 1239 (2001).
[30] I. Yonenaga. Mater. Trans. **46**, *9*, 1979 (2005).
[31] C. Claeys, E. Simoen. Fundamentals and Technological Aspects of Extended Defects in Germanium. Springer, Berlin, Heidelberg (2009). https://doi.org/10.1007/978-3-540-85614-6_1
[32] J. Lothe, J.P. Hirth. Phys. Rev. **115**, *3*, 543 (1959).
[33] A. George, J. Rabier. Revue Physique Appliquée **22**, *9*, 941 (1987).
[34] B.V. Petukhov, V.L. Pokrovskii. JETP Lett. **15**, *1*, 44 (1972).
[35] T. Ninomiya, R. Thomson, F. Garcia-Moliner. J. Appl. Phys. **35**, *12*, 3607 (1964).
[36] V.V. Rybin, A.N. Orlov. FTT **11**, *11*, 3251 (1969). (in Russian).
[37] B.V. Petukhov. Sov. Phys. Solid State **35**, *5*, 571 (1993).
[38] B.V. Petukhov. Phys. Solid State **66**, *3*, 458 (2024).

[39] O.M. Braun, Y.S. Kivshar. The Frenkel–Kontorova Model: Concepts, Methods, and Applications. Springer Verlag, Berlin-Heidelberg (2004).
[40] The sine-Gordon Model and its Applications / Eds J. Cuevas-Maraver, P.G. Kevrekidis, F. Williams. Springer, Switzerland (2014). https://doi.org/10.1007/978-3-319-06722-3
[41] P. Guyot, J.E. Dorn. Canadian J. Phys. **45**, *2*, 983 (1967).
[42] B.V. Petukhov, V.L. Pokrovskii. JETP **36**, *2*, 336 (1972).
[43] S. Flach, K. Kladko. Phys. Rev. E **54**, *3*, 2912 (1996).
[44] K. Kladko, I. Mitkov, A.R. Bishop. Phys. Rev. Lett. **84**, *19*, 4505 (2000).
[45] I. Mitkov, K. Kladko, A.R. Bishop. Phys. Rev. E **61**, *2*, 1106 (2000).
[46] O.V. Usatenko, A.V. Gorbach, A.S. Kovalev. Phys. Solid State **43**, *7*, 1247 (2001).
[47] J.R. Patel, P.E. Freeland. J. Appl. Phys. **42**, *9*, 3298 (1971).
[48] B.Ya. Farber, I.E. Bondarenko, V.I. Nikitenko. FTT **23**, *7*, 2192 (1981). (in Russian).
[49] P. Gall, J.P. Peyrade, R. Coquillé, F. Reynaud, S. Gabillet, A. Albacete. Acta Metallurgica **35**, *1*, 143 (1987).

Translated by E.Ilinskaya